npj | Climate and Atmospheric Science

www.nature.com/npjclimatsci

ARTICLE OPEN

Check for updates

Linkage between precipitation isotopes and biosphere-atmosphere interaction observed in northeast India

Supriyo Chakraborty[1,2]✉, Pramit Kumar Deb Burman[1,2], Dipankar Sarma[1], Nitesh Sinha[3,4], Amey Datye[1], Abirlal Metya[1], Charuta Murkute[1], Subodh K. Saha[1], Krishnakumar Sujith[1], Nirmali Gogoi[5], Abhijit Bora[5], Sabyasachi Maji[6], Dipak K. Parua[7] and S. Bera[7]

The intra-seasonal variation in precipitation isotopes shows a characteristic declining trend over northeast India. As of now, no mechanism offers a consistent explanation of this trend. We have performed the isotopic analysis of precipitation (rain) and estimated net ecosystem exchange and latent heat fluxes using an eddy-covariance system in northeast India. Additionally, we have used a diagnostic model to determine the recycled rainfall in this region. We find a strong link between the enhanced ecosystem productivity and isotopic enrichment in rainwater during the premonsoon season. Subsequently, on the advent of monsoon, the Bay of Bengal generated moisture enters this region and depletes the isotopic values. Additionally, the regional-scale convective activities produce periodic lows in the precipitation isotopes. Contrary to the general understanding, our study shows that the internal factors, such as the local land-atmosphere interactions, rather than the external influences, play a significant role in governing the precipitation isotopes in northeast India.

npj Climate and Atmospheric Science (2022)5:10 ; https://doi.org/10.1038/s41612-022-00231-z

INTRODUCTION

A variety of ocean-atmospheric processes controls the isotopic composition of precipitation. Since a significant amount of atmospheric water vapour is generated from the oceans, the physical conditions of the surface ocean leave their imprint on the isotopic composition of vapour and precipitation. Post-evaporation processes, such as the atmospheric circulation[1], condensation of vapour into raindrops[2], and their subsequent evaporation[3], rain–vapour interaction[4,5] also strongly affect the precipitation isotopic fractionation. Convective activity, moisture flux convergence, and cloud processes[6,7] also modulate the precipitation isotopic composition. Compared to oceanic production, the continental production of moisture is relatively small; however, it may be significant in specific areas depending on the bio-geographical condition.

The oxygen isotopic ($\delta^{18}O$) profiles of precipitation on an intra-seasonal timescale often show a declining trend in some parts of India, such as Ahmedabad[4], New Delhi, and Mumbai[8], Port Blair[9] in the Bay of Bengal (BoB) during the monsoon season (June to September). Such kind of declining effect is most dramatic in the northeast region of India (henceforth represented as NEI; Fig. 1a). For example, Breitenbach et al.[10] observed a decrease in $\delta^{18}O$ values ca. 15‰ at Cherrapunjee, Assam. Sinha et al.[11] reported $\delta^{18}O$ variations of Tezpur in NEI and observed a declining trend over 10‰. The cause of such depletion in $\delta^{18}O$ is believed to be the modulation by ocean-atmospheric processes. A shift in moisture source from the north BoB to the equatorial Indian Ocean[10] and large-scale planetary circulation was speculated[12] to explain the reducing trend in $\delta^{18}O$. Recently, Cai and Tian[13] invoked the concept of westerly and easterly circulations that produced higher and lower precipitation isotopic values, respectively, in the head Bay region. Their hypothesis, however, cannot explain the mechanism of generating the premonsoon high precipitation isotopic values. The reported Local Meteoric Water Line (LMWL) from NEI typically shows a slope like the Global Meteoric Water Line (GMWL; ~8) but intercept higher than 10‰[10,12]. This shows that a significant amount of recycled water vapour contributes to the local precipitation[14]. Earlier investigators mostly ignored the origin and role of this recycled water vapour.

Here we analysed several rainwater isotopes profiles from NEI, including a few other sites outside this region, to examine their intra-seasonal behaviour and find a more appropriate alternative explanation of this depletion. We propose that the land-surface processes mediated by plant transpiration play an essential role in controlling the precipitation isotopic behaviour during the preceding phase of monsoon in NEI. This produces a strong intra-seasonal precipitation isotopic gradient, denoted as LEMPIG (Late monsoon Early Monsoon Precipitation Isotope Gradient). The objectives of our study are: What processes control the isotopic variability of precipitation in NEI on an intra-seasonal timescale? Does plant physiology play any role in determining the precipitation isotopic composition? Whether the internal processes or the external factors play a significant role in modulating the precipitation isotope values in this region? We follow a multi-disciplinary approach to address these questions. First, we examine a comprehensive data set of precipitation isotopes from across this region and analyse the regional meteorological parameters. Second, we analyse the latent heat flux (LE) and net ecosystem exchange (NEE) measured by an eddy-covariance (EC) system, along with the reanalysis and observed rainfall data. Third, we estimate the recycled ratio (RR: ratio of recycled to the total rainfall) of rain on a seasonal scale to constrain the isotopic observations. To better comprehend the precipitation isotopic characteristic of NEI, we also present the isotopic data of another urban, semi-arid region in western peninsular India (Pune area). This region has a contrasting behaviour in terms of the moisture

[1]Indian Institute of Tropical Meteorology, Ministry of Earth Sciences, Pune, India. [2]Department of Atmospheric and Space Sciences, Savitribai Phule Pune University, Pune, India. [3]Center for Climate Physics, Institute for Basic Science, Busan, Republic of Korea. [4]Pusan National University, Busan, Republic of Korea. [5]Department of Environmental Science, Tezpur University, Tezpur, India. [6]Bose Institute, Kolkata, India. [7]Department of Botany, Calcutta University, Kolkata, India. ✉email: supriyo@tropmet.res.in

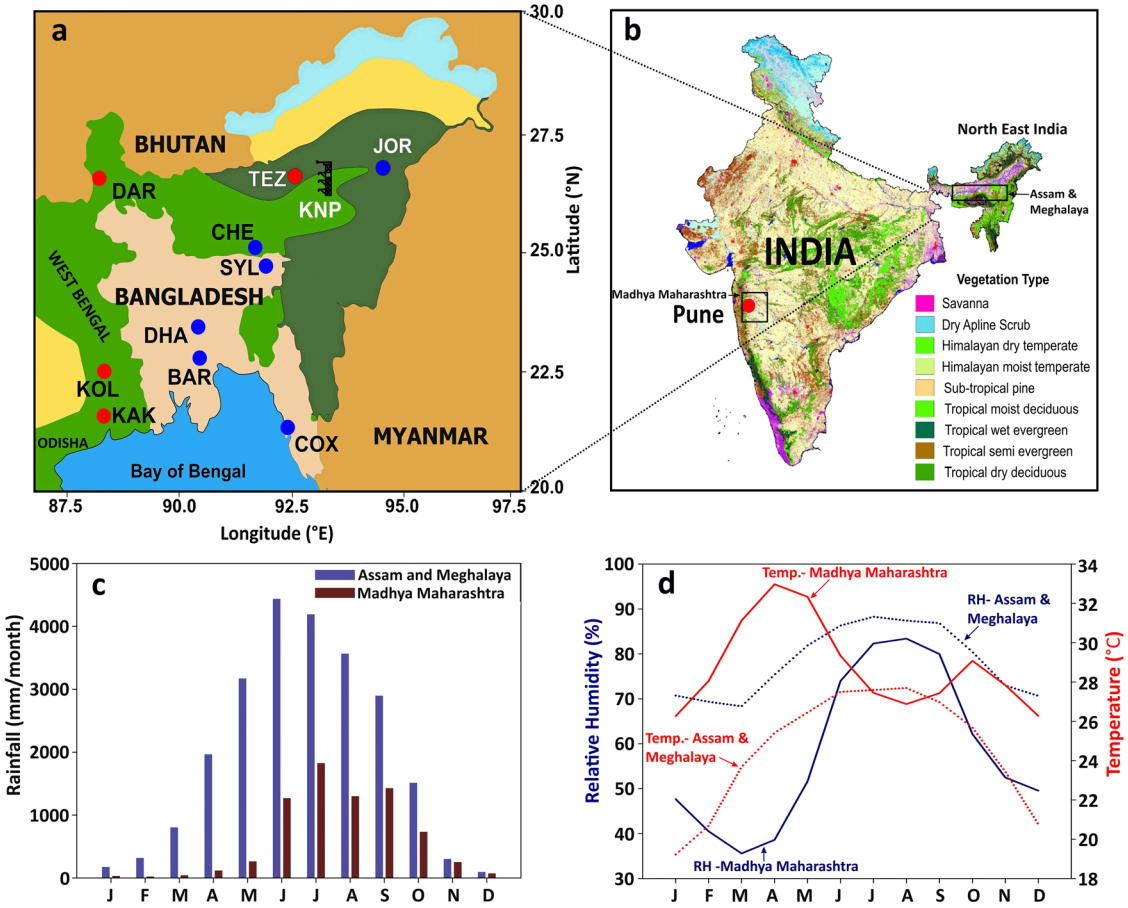

Fig. 1 Study area and site description. a Map of northeast India depicting the study area. The precipitation samples collection sites are Tezpur (TEZ), Darjeeling (DAR), Kolkata (KOL), and Kakdweep (KAK; all in red dots). The Kaziranga forest site (KNP) containing the eddy-covariance tower is shown. The published data of precipitation isotopes are available from Jorhat (JOR), Cherrapunjee (CHE), and the sites in Bangladesh (Dhaka, Sylhet, Barishal, and Cox Bazar; blue dots) are also shown in this map. **b** The India map and its vegetation types are illustrated. As revealed in this diagram, the forest cover in northeast India is much higher than the rest of the country. **c** The climatological (1871–2016) variation of rainfall on a monthly scale for Assam and Meghalaya (blue bar) and Madhya Maharashtra (containing the Pune city) (dark red bar) has been shown. **d** The monthly variations of temperature and relative humidity for the above mentioned two regions are also shown.

source, underlying land surface processes, and intra-seasonal variations of precipitation isotopes. Finally, we compare the precipitation isotopic behaviour of these two contrasting regions to further demonstrate the linkage between precipitation isotopes and biosphere–atmosphere interaction.

RESULTS

Characteristics of the precipitation isotopic profiles

Rainwater oxygen isotopic values for Tezpur and Darjeeling are shown in Fig. 2a, b, respectively. The patterns of all these profiles show relatively high values during the premonsoon season (March-May) and lower values during the late phase of monsoon (August-September). The isotopic values show low variability in both sites until May; afterwards, they show significantly large variability. For Tezpur, the $\delta^{18}O$ values approximately range from +2 to −18‰. Darjeeling shows a higher range, from +3.5 to −21‰. Apart from their decreasing pattern, the isotopic profiles showed pulses of high negative values (grey bars; Fig. 2).

Figure 2c shows the general behaviour of precipitation $\delta^{18}O$ representative of NEI (see Supplementary Note 1). Isotopic values are enriched (≈1‰) during the early part of the year and then decrease progressively. We observed a sharp decrease in June (average value: ~−4‰). The $\delta^{18}O$ values decrease and achieve the minimum value ca. −10‰. Subsequently, $\delta^{18}O$ rises and remains approximately −4‰ in November-December.

We have also plotted an LMWL (Fig. 2d) representing this region. The slope and intercept of this line are 8.02 ± 0.08 and 13.02 ± 0.53‰, respectively (summarised in Supplementary Table 1).

We show the slope and intercept values calculated on a monthly timescale in Fig. 2e. The area receives significant rainfall in May. As a result, the humidity level goes up (≥80%, Fig. 1d), which helps the slope to increase from a low value of ~6.9 in April to ~7.8 in May. Monsoon sets in June (see Supplementary Table 2), and the humidity is further increased, so is the slope (~8.2). Subsequently, the slope is reduced and maintains 7.8 to 7.6 in the remaining monsoon season. We quantify the LEMPIG as the difference between the average values of $\delta^{18}O$ in March–April and September–October for a specific site.

Biosphere–atmosphere interaction

It is a fact that the photosynthesis by plants is strongly coupled with their transpiration process[15]. An enhanced rate of carbon assimilation usually favours an increased rate of transpiration. Our earlier work on the EC-based estimation of biosphere-atmosphere CO_2 fluxes in the Kaziranga National Park (KNP) reveals maximum photosynthetic carbon assimilation during the premonsoon

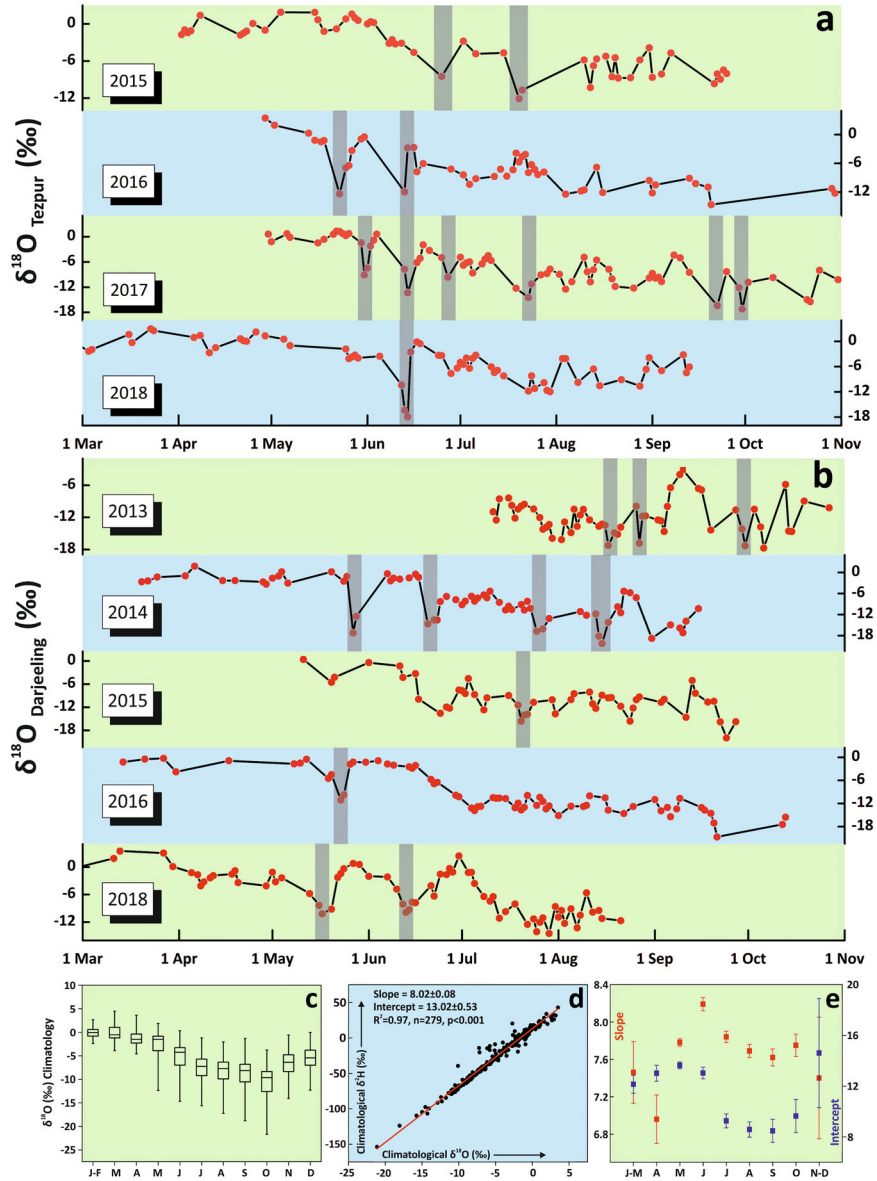

Fig. 2 Precipitation isotope records. Multi-year oxygen isotopic precipitation records for Tezpur (**a**) and Darjeeling site (**b**), respectively. Lower panel **c**: box plot of the climatological variation of $\delta^{18}O$ for north-east India; **d** meteoric water line for NEI. **e** Monthly variation of NEI meteoric water line slope (red dot) and intercept (blue dot). Error bars indicate standard deviation.

season[16,17]. In the present study, we have analysed the EC-based CO_2 fluxes to determine the diurnal variation of NEE on a monthly timescale during 2016–2018 (a detailed discussion of the EC results is presented in Sarma et al.[18]).

Seasonal variation of recycled rain (RR)

It is known that NEI receives considerable rainfall through recycled moisture. Chowdhury et al.[19] examined this behaviour on a climate scale (1979–2014) for the monsoon season. They showed that about 7% of total rainfall during the monsoon season is contributed by local moisture supply (i.e., evapotranspiration (ET)). Here we have done a similar exercise, but for each season (DJF: winter; MAM: premonsoon; JJA: monsoon; and SON: postmonsoon) separately to examine the seasonal evolution of recycled rainfall). It is clear from this estimate (Supplementary Fig. 1) that the contribution of recycled rainfall to precipitation is minimum during the monsoon season (June to September). Then it progressively increases and reaches a maximum during the winter (November–December). After that, it slightly decreases, still maintains high values until the premonsoon season. The monsoon sets in around June, and marine water vapour enters the region. As a result, the proportion of recycled moisture in rainfall decreases.

DISCUSSION

Figure 2a, b show the general characteristics of precipitation isotopic variability at the Tezpur and Darjeeling sites, respectively. The range of isotopic fractionation at Darjeeling is considerably higher than that observed at Tezpur. Since Darjeeling's (2186 m) elevation is much higher than that of Tezpur (48 m), the isotopic values are more depleted at the former site due to the 'altitude effect'[20]. Figure 2c shows the climatological variation of $\delta^{18}O$ over NEI. We observe relatively higher values of $\delta^{18}O$ from January to May because of the ET-derived moistures; we will discuss this in the subsequent sections. With the advent of the monsoon season in June, a sharp drop in the isotopic values is observed. Figure 2d

shows the LMWL representing the entire NEI region. The slope (8.02 ± 0.08) of this LMWL is the same as that of the GMWL. Still, a slightly higher value of intercept (13.02 ± 0.53) suggests a relatively higher proportion of ET-derived water vapour in this region. High humidity during the monsoon season helps maintain a slope value of 8.0 ± 0.2. During the late winter and spring, the slope is typically lower than 8, showing kinetic fractionation. During the postmonsoon season, the humidity level drops, and the proportion of ET-generated moisture increases, resulting in a slight rise in isotopic values. Hence, the slope decreases to some extent.

Similarly, the intercept shows a relatively high value in the early year, representing significant secondary moisture contributing to the rainfall. The high influx of marine water vapour during the monsoon causes the intercept and its variability to decrease. The intercept increases again in the postmonsoon because of the admixture of moisture from multiple sources. The patterns of slope and intercept of the LMWL, show consistent behaviour with the RR estimation.

During the premonsoon season, NEI receives abundant rainfall due to the thunderstorm activities[21], because of this, the soil water content increases. The photosynthetic activity is enhanced and so is plant transpiration. To track the photosynthetic activity, the EC-derived net carbon fluxes are plotted in Supplementary Fig. 2, which illustrates that the maximum carbon uptake (CO_2 flux from the atmosphere to biosphere ~20 μmol m^{-2} s^{-1}) takes place during the premonsoon season. On the other hand, the minimum carbon transfer (~6 μmol m^{-2} s^{-1}) is observed during the winter (Supplementary Fig. 2). The meteorological condition drives the seasonal carbon uptake characteristics of the KNP ecosystem. Deb Burman et al.[17] analysed the photosynthetic photon flux density on a seasonal scale and concluded that the photosynthesis and ET are most and least strongly coupled in the premonsoon and winter seasons, respectively. Hence, the transpiration process of the forests in this region, interlinked with their carbon uptake, is expected to leave its signal on the precipitation isotopes of this region.

Further, the EC-based observations at KNP show that the LE is maximum during May–June[16,18]. The monthly LE estimated on a regional scale shows a peak in May and another slightly smaller peak around September, driven by the enhanced transpiration; (Supplementary Fig. 2; also see the Supplementary Note 2 depicting the relationship between the LE derived from the EC system and the ERA5 reanalysis data). It is to be noted that the precipitation $\delta^{18}O$ also shows higher values during early May, which coincides with the high transpiration flux (~3.5 mm d^{-1}) (Supplementary Fig. 3a). It is well known that an enhanced soil evaporation rate makes the remaining soil water isotopically enriched[22]. This isotopically enriched water, when ingested by plants, the transpired water also becomes isotopically enriched[22]. However, during the heavy rain condition, due to the reduced rate of soil evaporation, the isotopic composition of transpired water would be close to that of the rainwater[23]. A similar situation prevails in NEI during the premonsoon season.

On the other hand, a higher amount of secondary moisture does not necessarily yield enriched oxygen isotopes. This is because the evaporation of soil water releases isotopically depleted water vapour into the atmosphere[22]. So, the enrichment of ^{18}O in precipitation must originate from an enriched source of moisture, which in this case can only be obtained from the high amount of transpired water vapour. The appearance of the second peak in LE (~105 W m^{-2}) during the latter phase of monsoon (Supplementary Fig. 2) shows an increased ET (~3.8 mm d^{-1}; Supplementary Fig. 3a), which although is unlikely to be associated with an increased number of heavier isotopes. This is clear in the progressively decreasing values of precipitation $\delta^{18}O$.

The increased abundance of heavier isotopes during the premonsoon season and its lower proportion during the monsoon season could also be investigated by analysing the dependence of $\delta^{18}O$ on LE. The LE is generated when the water is vapourised, driven by evaporation and transpiration. Since the evaporation releases lighter isotopes faster from the soil surface, the precipitation isotope is expected to show an inverse, albeit weak, correlation with the LE. If the proportion of heavier isotopes were increased, the pattern of $\delta^{18}O$–LE correlation would change. The inverse relationship is likely to become neutral or weakly positive. Our investigation shows that, in general, the precipitation $\delta^{18}O$ is negatively correlated with the LE averaged on a daily timescale. Figure 3 shows the scatter plots between the LE and precipitation isotope data. We chose the Tezpur site isotope record because of its proximity to our EC tower location. In this context, we like to emphasise that the $\delta^{18}O$ and LE would show a strong correlation when the entire amount of water vapour emitted through the ET process is condensed and precipitated as rainfall, i.e., ET and precipitation, make a closed system. Since such a scenario is not possible on a local to regional scale, $\delta^{18}O$ and LE would only show a weak correlation. Such a weak correlation characterises the monsoon season. But since the premonsoon season releases a relatively more number of ^{18}O than the monsoon season through transpired water vapour, the LE–$\delta^{18}O$ correlation during this time not only increases but also turns positive. The change in sign of the correlation value (Fig. 3e, f) provides firm support for our hypothesis; i.e., premonsoon season releases a greater number of ^{18}O through the ET process.

Further, we have 1 year (2016) of data available near the tower site (~1 km off the tower), which has also been used for this LE–$\delta^{18}O$ analysis (Fig. 3a). Each year but 2017, shows an inverse correlation. In 2017, the EC system failed from mid-June to September. As a result, we could not get the LE data, and hence the LE, $\delta^{18}O$ paired data were not available for the above period, yielding fewer data points during the monsoon season this year.

To examine the behaviour of LE and $\delta^{18}O$ interrelation on a seasonal timescale, we have compiled the LE, $\delta^{18}O$ pairs available for all the years comprising premonsoon and monsoon seasons. The winter and postmonsoon seasons are excluded because of the scarcity of data. As shown in Fig. 3e, the LE–$\delta^{18}O$ correlation during the MAM season shows a gentle increasing trend. The same in the JJA season shows a moderately declining trend (Fig. 3f). The positive trend observed during the MAM season provides firm evidence of an increased number of heavier isotopes (^{18}O) because of enhanced transpiration. Subsequently, the negative trend observed during the monsoon season implies a drop in the number of heavier isotopes but an increase in the lighter isotopes (^{16}O) because of the incursion of the marine water vapour, depleted in isotopic value.

The parameters mentioned above in 2017 show a weak positive trend; moreover, most of the samples in this year belonged to April and May, some samples to June, and only a very few samples to September. So, this result attests to our hypothesis that the premonsoon time releases a relatively greater number of heavier isotopes through the ET process. It is to be noted that the role of the ecosystem in producing enriched isotopic values during the premonsoon season is also supported by the analysis of remote sensing data[24].

The climatological variations of ET and T (transpiration) (Supplementary Fig. 3a) show that the T is maximum during late April and early May; subsequently, T decreases steadily. As mentioned earlier, an enhanced rate of soil water evaporation leads to the enrichment in soil water isotopic composition and is manifested in the transpired water vapour. Supplementary Fig. 3b shows the monthly climatology of the soil water content at the surface (0–10 cm) and the root zone (10–800 cm) for this area (obtained using the Global Land Evaporation Amsterdam Model (GLEAM)[25] output). As depicted in this figure, the soil water content during March shows a minimum value; subsequently, it increases sharply, facilitating rapid evaporation. With the advent

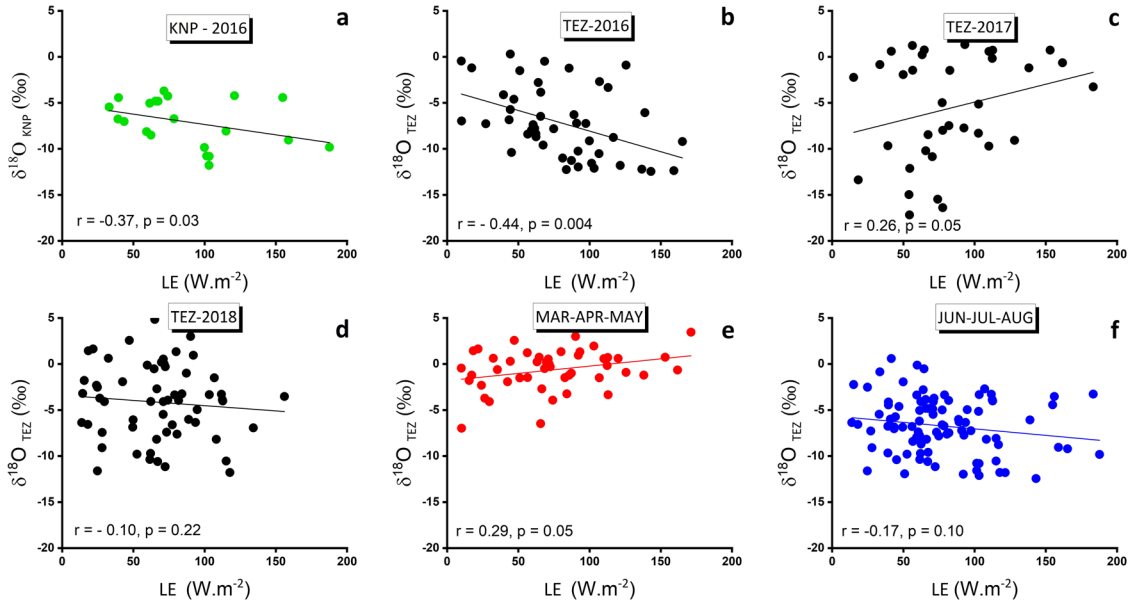

Fig. 3 Relation between latent heat flux and precipitation $\delta^{18}O$. Scatter plots for LE and precipitation $\delta^{18}O$ for **a** Kaziranga forest (the year 2016), water sampling site was close to the eddy-covariance tower (~1 km). **b** Tezpur site (year 2016), **c** Tezpur site (year 2017), **d** Tezpur site (year 2018). Barring 2017, in general, an inverse correlation was found in all the cases. The remaining plots in the lower panel show the same scatter plot but on a seasonal time scale combining all year data. **e** Premonsoon (March–April–May) and **f** monsoon (June–July–August) seasons. A positive trend in MAM is indicative of the presence of an increased number of heavier isotopes (^{18}O) in the water vapour flux relative to that of the JJA season.

of the monsoon season, the soil water evaporation rate reduces; hence the transpired water vapour produces relatively depleted isotopic values. Afterwards, soil water decreases moderately during the postmonsoon season. The occurrence of heavy rain during the monsoon season and subsequent retention of a high amount of soil water even during the postmonsoon season does not allow soil water to be isotopically enriched. Considering the rainfall recycling, a higher fraction of evaporated water vapour than the transpired water vapour causes relatively higher RR during the postmonsoon season. The transpired water vapour fraction using the GLEAM data indeed supports this assertion. Hence, the transpired water vapour during the monsoon and postmonsoon seasons cannot produce isotopically enriched rain compared to the premonsoon season.

We have calculated yet another parameter, the canopy-atmosphere decoupling coefficient (Ω, dimensionless) to describe the relative roles of biospheric and environmental processes in controlling the total water vapour exchange at our study site. The ET primarily comprises transpiration, a biologically controlled water vapour flux governed by plants' stomatal opening and closure. The second component is evaporation, a physical vapourisation of water. In the absence of the separate measurements of these components, we use Ω to infer the relative controls of these two parameters on the ET at KNP. Ω has been defined as the ratio of environmental to physiological controls of ET[15] (vide the 'Methods' section for details). Lower values of Ω signify the greater contribution of transpiration in ET and higher values of Ω stand for the increased role of evaporation in ET. As detailed in Deb Burman et al.[26], Ω is lower (~0.25) in premonsoon (MAM), highlighting increased transpiration during this season. Further, Ω is higher (0.35) in monsoon (JJA), showing that evaporation is the principal contributor to LE in this season. Overall, these findings support our isotope-based observations.

As mentioned earlier, several lows characterise the isotopic values during the monsoon season. Such periodic low values have been observed at several places and are believed to be associated with intense convective activities[27,28]. But the atmospheric controls of precipitation isotopes on intra-seasonal timescale at NEI and other Indian sites, such as the coastal region of Kerala[28] may not be the same. The mean residence time of moisture in the atmosphere is over a week[29]; the cumulative outcome of these convective processes imparts a 'memory effect' resulting in a declining trend in the precipitation isotopes in NEI. But unlike NEI, a strong monsoonal circulation heavily influences the coastal and inland areas of Kerala[28]. As a result, the memory effect of the isotopic depletion is not sustained, which helps to get back the isotopic 'background' value relatively quickly. So, the condition to have a significant LEMPIG is that the area under consideration should be relatively free of external atmospheric influences.

Distinct low values also characterise the isotopic rainfall values in the head BoB region and possess a declining trend. However, it may be noted that the sea surface temperature forcing provides the major amount of moisture and drives the convective activities in the north BoB region[30,31]. On the other hand, orographic influence and land surface processes strongly affect the precipitation in the continental area of NEI. Because of these different feedback mechanisms, the isotopic depletion observed in the coastal region (Kolkata and Kakdweep) is characteristically different from that found in NEI. The interaction between the oceanic moisture and that generated through the land-surface processes and its modulation by the regional-scale convective activities and moisture recycling determine the isotopic composition of precipitation in NEI.

In NEI, convective events are triggered when the environment is sufficiently moisture-loaded and strong vertical winds carry moist air parcels aloft. In general, strong precipitating convection is expected in moist atmospheric conditions[32,33]. We have used the vertical wind speed (w-wind) data of the KNP tower site to examine whether higher wind speed, a proxy for convective activities[34], is associated with the lower isotopic values. Figure 4 shows the variation of $\delta^{18}O$ and w-wind observed at Tezpur during premonsoon to postmonsoon, for three years (2016 to 2018) of our study. The associated rainfall events obtained from the multi-component weather sensor at KNP are also shown (blue bars). In the case of 2016, the higher w-wind values are usually associated with the low $\delta^{18}O$ values, though in one case (May 15,

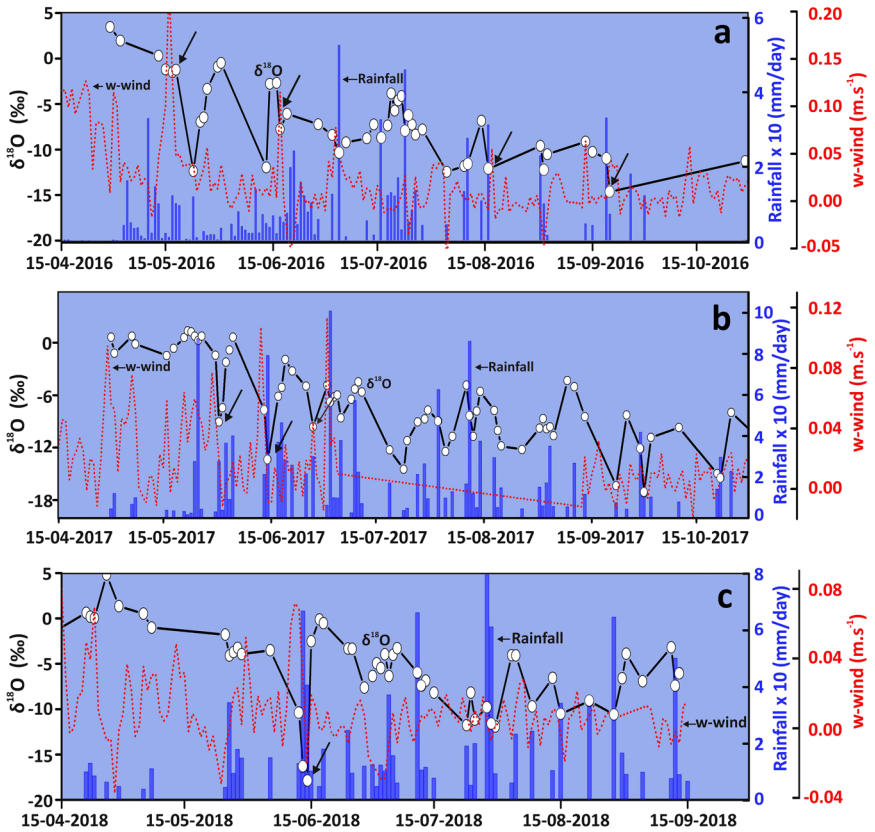

Fig. 4 Co-variability of Tezpur precipitation $\delta^{18}O$ and the w-wind. The daily time-series plots show the co-variability of $\delta^{18}O$ and the w-wind parameters for years **a** 2016, **b** 2017, and **c** 2018 for the Tezpur site. The link between the isotopic lows and the vertical wind speed represents the convective processes. The diagonal arrows are marked where low isotopic values are associated with high w-wind. Blue bars show the daily rainfall amount.

2016), $\delta^{18}O$ lagged high w-wind by about a week. But in most other cases, the low $\delta^{18}O$ values occur near-synchronously with the high vertical wind. We observed similar behaviour in 2017 as well. Isotopic depletions follow three high w-wind events. Due to the non-functioning of the sonic anemometer, no wind data was available from the first week of July to the end of August. Hence, we could not examine this behaviour during this period in 2017. But again, in September, one such event was observed. In 2018, one large depletion in $\delta^{18}O$ was associated with a high w-wind value. However, several high w-wind values were observed during March and April in 2018, but due to low moisture loading, sufficient convection could not take place[32]. Hence, isotope values did not suffer significant depletions.

The association between high w-wind speed and rainfall $\delta^{18}O$, operating within a spatial scale of ~50 km, shows that the local-scale processes significantly influence the isotopic depletions. To examine the effect of monsoon circulation, which operates on a much wider scale, we analysed the impact of moisture transport fluxes over the study region. The scaling of moisture transport in NEI is explained in Supplementary Note 3.

We calculated the vertically integrated moisture transport (VIMT) to examine the effect of moisture transport and regional scale convective activities on the precipitation isotopes, specifically for the monsoon season. This is depicted by the time-latitude Hovmöller diagrams of the average of National Oceanic and Atmospheric Administration (NOAA) interpolated outgoing long-wave radiation (OLR) anomaly in the backdrop of the isotopic profiles. Figure 5 shows the results for 2015 and 2016, while the same for 2017 (Supplementary Fig. 4) and 2018 (Supplementary Fig. 5) are presented in the Supplementary Information section.

The co-occurrence of the isotopic depletions with high VIMTs indicates the influence of the monsoon-induced moisture transport on the precipitation isotopes. In 2015, out of three intense VIMT events (see arrows), two events did not show any link between high VIMT and depleted isotopic values. A significant isotopic depletion took place in the last week of July. During this time, a deep depression formed in the north BoB (on 27 July, 2015), which intensified into a severe cyclonic storm Komen[35]. On July 30, very heavy rainfall was reported in Bangladesh and India. As a result, the coastal site of Sundarbans experienced a drop in $\delta^{18}O$ by ~12‰ within a week.

We also observed a near synchronous reduction in $\delta^{18}O$ in Kolkata and Barisal. However, the $\delta^{18}O$ values at Darjeeling indicated that the Komen isotopic signature did not propagate toward the north, as no clear signature of this cyclone was observed (in Fig. 5a). The $\delta^{18}O$ profile steadily decreased from the high values in premonsoon to the low values in the late monsoon with a LEMPIG of 12.5‰. The Tezpur site also did not show any Komen signature in its precipitation isotopes. Hence, the isotopic anomaly created by this cyclonic event was confined within its spatial extent (~100–200 km). We also examined the propagation of the rainfall anomaly further north. The right panel in Fig. 5a shows a high positive rainfall anomaly over the coastal region, but the anomaly hardly reached farther north. As a result, no high isotopic depletion was observed in Darjeeling or Tezpur. However, the regional-scale convective activities could occasionally cause concurrent low values in the precipitation $\delta^{18}O$. For example, a near synchronous negative $\delta^{18}O$ anomaly occurred in all the sites during the fourth week of June. The convective activities spreading across this region caused the depletion, as revealed in the Hovmöller diagram of the interpolated OLR (Fig. 5). The VIMT

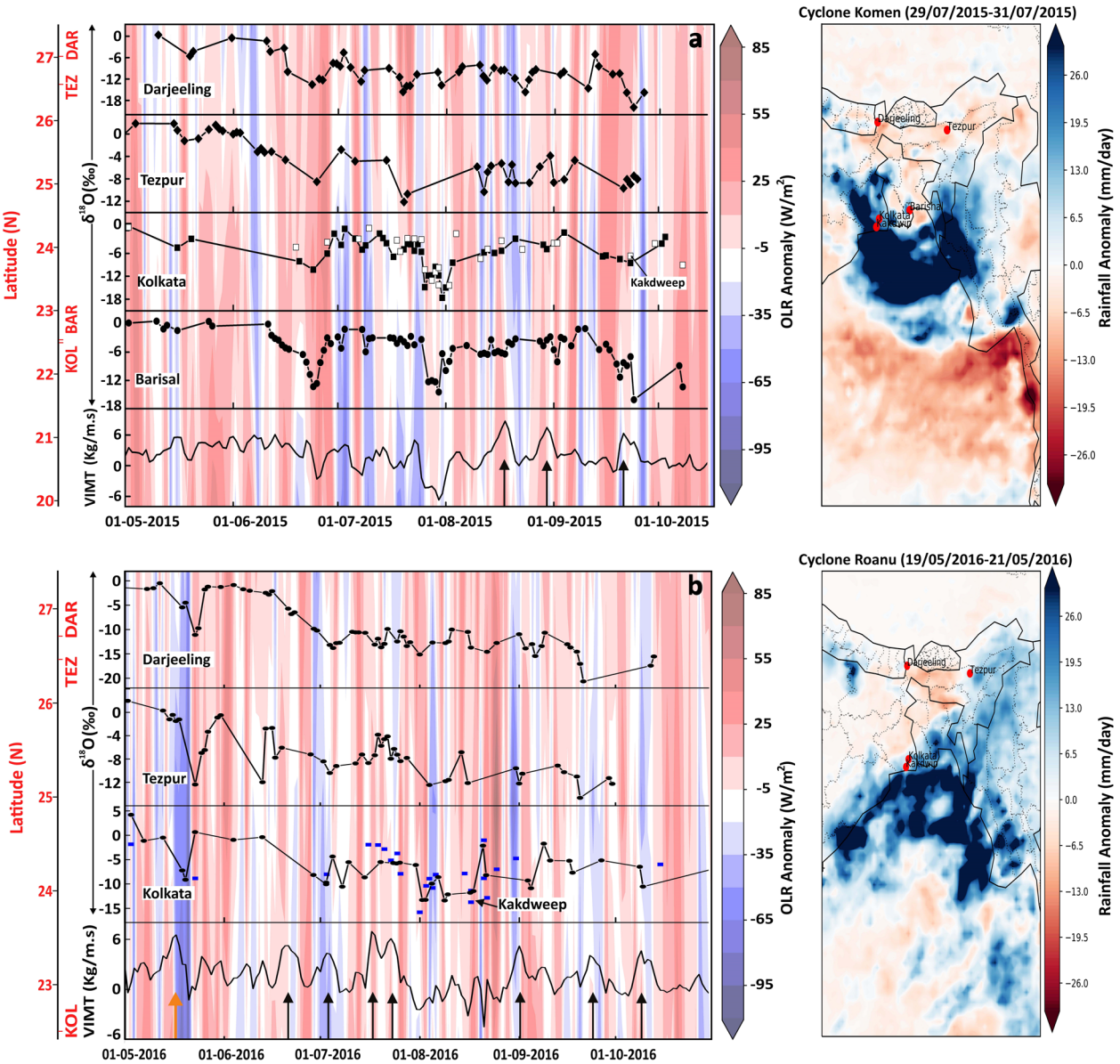

Fig. 5 Precipitation isotopes and convective activity. Relation between the precipitation isotopes (lines) and convective activities (represented by shading; the OLR anomaly) are shown. **a** The link between the vertically integrated moisture transport/convective events and the precipitation isotopes at four sites, Kolkata, Tezpur, Darjeeling, and Barisal. The Kakdweep data (white boxes) is also shown along with the Kolkata record. The upper right panel shows the rainfall anomaly observed during a cyclonic event 'Komen' during which high VIMT was found. But the anomaly had little effect either at Darjeeling or Tezpur. **b** The same as above but for the year 2016. Similar behaviour was observed concerning the control of the VIMT on the precipitation isotopes. A regional-scale convective activity (shown as an orange arrow at the bottom panel) happened soon after a deep depression (Roanu) around May 20 (lower right panel), which caused near synchronous precipitation isotopic depletions in all three sites.

showed a slightly high value during this time. Another low-intensity convective activity took place in the second week of July.

We observed smaller $\delta^{18}O$ depletions at some sites but did not find a concurrent high VIMT. Similar behaviour is observed in 2016 as well, in which the isotopic profiles at Kolkata (including Kakdweep), Tezpur, and Darjeeling are examined (Fig. 5b). It is evident from this plot that the high VIMT values did not always associate with the low precipitation $\delta^{18}O$. However, one distinct low $\delta^{18}O$ was observed in all three sites in the third week of May. On 17 May 2016, the VIMT showed a high value. In the subsequent days, all three sites experienced low $\delta^{18}O$. For example, the Kolkata, Tezpur, and Darjeeling sites had low $\delta^{18}O$ values on 20, 23, and 24 May. The negative excursion of $\delta^{18}O$ at Kolkata was caused by a deep depression *Roanu*. However, its associated rainfall was not significantly observed at far distant sites in Darjeeling and Tezpur. We calculated the rainfall anomaly during this event and observed its spatial distribution across the region to further check this assumption. As shown in Fig. 5b (right panel), a high positive rainfall anomaly existed in the coastal area of north BoB. The rainfall anomaly weakened considerably towards Tezpur, and practically no such effect was observed in Darjeeling. But it is interesting to note that a high w-wind at the KNP site was observed just before this event (Fig. 4a), which acted as a precursor of a regional scale convective activity. Around the same time, the VIMT also showed an increased value (see the orange arrow in Fig. 5b lower panel), and OLR reduced considerably, as evident in the OLR anomaly plot. As a result, the precipitation $\delta^{18}O$ registered a near-synchronous depletion across the region.

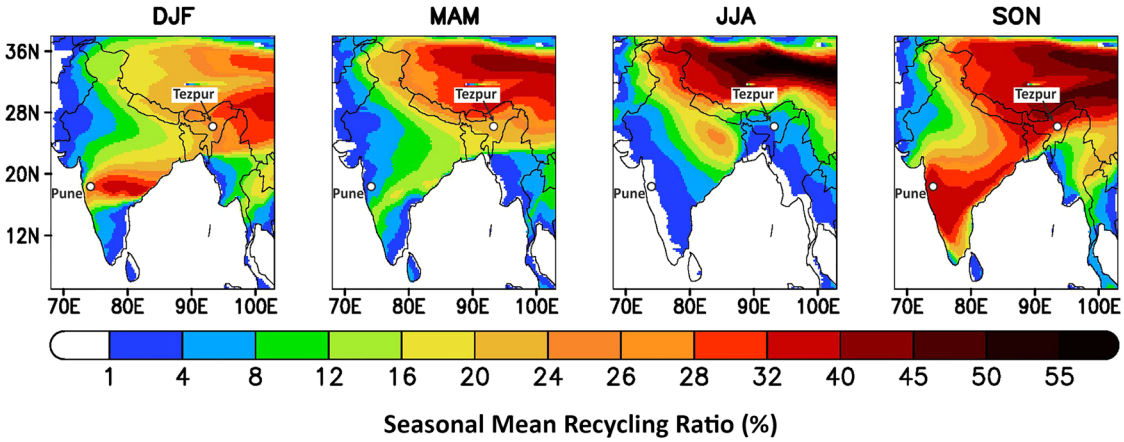

Fig. 6 Recycling ratio. The seasonal mean recycling ratio (recycled to total rainfall in %) estimated using ERA5 data (2014–2018) by employing the recycling model of Eltahir and Bras[43].

In 2017, the Tezpur site recorded six or seven low $\delta^{18}O$ events (Supplementary Fig. 4). Still, those are not caused by the regional scale convective activities, as revealed by the OLR anomaly plotted on a Hovmöller diagram. Instead, some of the low $\delta^{18}O$ values seem to be associated with high w-wind. For example, −7‰ in mid-June 2016, −12‰ in mid-August 2016, −9‰ in May 2017, −14‰ in June 2017, and −17‰ in June 2018 (Supplementary Fig. 5) typically correspond to the high w-wind values as depicted in Fig. 4. An increase in the w-wind values shows the influence of the local-scale convective activities (as described in the previous section). A regional-scale convective event was observed in the middle of May. But as depicted in the $\delta^{18}O$ plots, no significant drop in $\delta^{18}O$ was observed at any of these three sites. By the end of May, a severe cyclone *Mora* developed in the north-central BoB, making landfall near Chittagong in Bangladesh (approximately 500 km east of Kolkata). During this event, the rainfall anomaly (Supplementary Fig. 4 right panel) and the rainfall isotopic records of Kolkata and Tezpur (Supplementary Fig. 4 left panel) show Tezpur to experience moderate rainfall. As a result, the isotopic values were reduced to about 6‰ relative to the preceding days, but the Kolkata site suffered from no such isotopic depletion.

In 2018, the isotopic profiles at Tezpur and Darjeeling (Supplementary Fig. 5) showed a concurrent low $\delta^{18}O$ event around the middle of June. Though the Kolkata site also experienced depleted isotopic values around the same time. The extent of depletion was not significant, implying that the convective activity was confined to the limited areas in the northern part of NEI. During the third week of July, heavy rainfall in Kolkata caused high isotopic depletion, the effect of which was observed at Darjeeling. Still, a moderate effect was observed on the precipitation isotopes in Tezpur, implying the absence of widespread convective activity across the region.

Northeast India is characterised by a humid climate and harbours rich forests. In contrast to NEI, the Pune city (18.5°N, 73.8°E) is a semi-arid site in western India. In this section, we have compared the isotopic records of these two regions. We have evaluated the variation of the $\delta^{18}O$ record[23,36] (Supplementary Fig. 6) of Pune from 2014 to 2017. We examined its pattern of intra-seasonal variation. Until the middle of the monsoon, the moisture comes primarily from the Arabian Sea. From September, the marine component decreases, but the ET-derived moisture increases. The climatological variation of evaporation and transpiration for the Pune region (Supplementary Fig. 6, lower panel) shows low ET-generated moisture until the middle of May. After that, its contribution steadily increases, driven by the premonsoon showers, resulting in the fluctuation in the isotopic value (grey shaded ellipse). A steady flow of moisture from the Arabian Sea causes rainfall in early June, reducing the isotopic values. But from the latter part of August, the fluctuation in $\delta^{18}O$ increases due to the increased proportion of ET-derived vapour (Supplementary Fig. 6, lower panel). We estimated the seasonal mean RR for this region to be about 30% during the postmonsoon season (Fig. 6), which caused large variability in its isotopic values. Unlike NEI, the $\delta^{18}O$ profile did not show any declining trend in the case of the Pune site. But raindrop evaporation caused an increase in the isotopic values and lowered the slope of the LMWL compared to the GMWL. For example, the slope of Pune LMWL (7.18; see inset in the upper panel of Supplementary Fig. 6) is considerably lower than that of the NEI-LMWL (8.02; Fig. 2).

Figure 6 shows the spatial variation of RR across India, generated using the ERA5 reanalysis data. This map shows that the RR during the MAM season is minimal in western peninsular India, including the Pune site (1–4%), but reasonably high (24–32%) for the NEI. This means that the evaporated and transpired moisture sources are small in western peninsular India. Hence, this region receives scanty rainfall during the premonsoon time, which is in sharp contrast to NEI (Fig. 1c).

In NEI, the isotopic variability of rainfall shows a decreasing trend superimposed with the periodic low values throughout the monsoon season. During the premonsoon season, the precipitation isotopic values remain reasonably high, driven mainly by the land-surface processes mediated by enhanced plant productivity. High radiation level, adequate rainfall, optimum soil water content trigger the photosynthetic activity, enhancing the transpiration process that produces moisture rich in heavier isotopes.

During the second phase associated with the monsoon onset, the BoB generated water vapours depleted in heavier isotopes sweep across this region. The extent of ET-derived water vapour is reduced. Local to regional-scale convective activities produce anomalous depletions in isotopic values. The convective events produce a significant water vapour depleted in the heavier isotopes (^{2}H and ^{18}O). Further, the secondary effects, such as the recycling of water vapour within the convective cells, reduce the rainwater's heavy isotopic composition during the convective events.

Our study shows that the isotopic values of precipitation in this region get modulated mostly by the land-surface processes; external factors play a secondary role in this regard. The study reveals that the hydrological processes which control the precipitation isotopic composition on an intra-seasonal timescale are relatively insulated from the external influences over the NEI region. During the monsoon season, the rainfall in NEI has been

rapidly decreasing for the last few decades. The extent of recycled rain is also experiencing a reducing trend in this season[17]. Though a similar analysis for the premonsoon season is not yet available, the long-term rainfall pattern during the MAM season shows a declining trend. This is especially significant for March because this is the time when an enhanced hydrological cycle triggers the primary productivity. Analysis of the rainfall data (1871–2016) for Assam and Meghalaya reveals that rainfall during March decreased approximately at a rate of 1.66 mm y^{-1} (see Supplementary Note 4). The RR for the MAM season in NEI is about 25% (see Fig. 6), the highest in India. A reducing trend in rainfall may have severe consequences for ecosystem productivity. This study shows a strong coupling between the hydrological cycle and the plant physiological processes during the premonsoon season. So, a declining trend in the RR may indicate the reduction of primary productivity, which may alter the carbon balance of the fragile ecosystems of northeast India.

METHODS

Sampling and isotope analysis

We collected rainwater daily at four sites; Tezpur (26.63°N, 92.80°E; 48 m above mean sea level (AMSL)) in the state of Assam, Darjeeling (27.04° N, 88.26° E; 2042 m AMSL) in West Bengal, Kolkata (22.57°N, 88.36°E; 9.14 m AMSL) in the southern part of West Bengal and Kakdweep (21.87°N, 88.18° E; 4 m AMSL) in the coastal region of the Sundarbans in West Bengal. Figure 1 shows a map depicting NEI and Bangladesh with the above-mentioned sites marked as red dots. Blue dots in this figure represent the study sites of other investigators. Rainwater samples were collected using ordinary rain gauges, providing the rainfall amount. This data, however, was not available for Kakdweep, Darjeeling 2017, and part of Darjeeling 2013 and 2016. We also collected rainwater for isotope analysis near the tower site (~1 km apart) in 2016. However, due to logistic difficulties, we could not continue the sampling in the subsequent years.

The sample collection time was typically 8:30 LT (local time). After collection, we transferred samples to leak-proof polypropylene vials of 15 ml size and then shipped them to the Indian Institute of Tropical Meteorology, Pune, for isotopic analysis. We used a liquid water isotope analyser (Model: TIWA-45-EP of the Los Gatos Research, USA) to measure the isotopic ratios with a precision of 0.12‰ and 0.8‰ for $\delta^{18}O$ and $\delta^{2}H$, respectively. While the uncertainty for d-excess, defined as $\delta^{2}H - 8 \times \delta^{18}O$ was 1.0‰.

Study area

The climate of NEI is quite distinct compared to the rest of India. This region receives very heavy rainfall, with several places being among the wettest in the world[19]. For example, the mean annual rainfall in NEI is 151.3 cm; the premonsoon time (March–May) witnesses a significant amount of rainfall driven by the thunderstorm activities[19], which is scanty in most other parts of India. A large portion of NEI is forest-covered (64%), much higher than the national average of India (Indian Forest Service; https://ifs.nic.in; see Fig. 1b; adapted from ref. [37]). According to the Köppen classification, the climate in this region is humid sub-tropical (CWa). The climatological (1871–2016) distribution of rainfall (the Indian Meteorological Department or IMD's rain gauge data available at www.tropmet.res.in were used) on a monthly scale for the two states of NEI (Assam and Meghalaya; a meteorological sub-division defined by the IMD) has been shown in Fig. 1 (lower panel). The same for the Madhya Maharashtra meteorological sub-division covering the Pune region is also shown for comparison purposes. The temperature and relative humidity of these two regions are shown in Fig. 1d. These figures show that the NEI region receives much higher rainfall, maintains a lower temperature, and has higher humidity than the Pune region.

EC data

Under the MetFlux India Project[38], we installed a flux tower at the Kaziranga forest (26.58°N, 93.10°E) to quantify the biosphere-atmosphere carbon exchange process, located approximately 50 km east of Tezpur. A micro-meteorological tower consisting of an EC system was set up in this location that measured CO_2 and water vapour concentrations using an enclosed path infrared gas analyser or IRGA sensor (Model: 7200, Li-COR Biosciences, Lincoln, USA).

This observational programme's instrumentation and analysis details are presented in[16,17]. This EC system's LE data (2016–2018) have been used[16] to interpret the precipitation isotope data.

Reanalysis data and GLEAM model output

To examine the behaviour of the LE over a broader scale, we have prepared the monthly climatology of the LE for 2014–2018 using the ERA5 reanalysis data for an area of 23°N–28°N, and 89°E–95°E. Then the CO_2 flux has been superposed on the LE values (Supplementary Fig. 2) to visualise their combined behaviour. The basic technique of calculating the CO_2 fluxes is presented in Sarma et al.[16].

We have used the ERA5 reanalysis data[39] to study the ET characteristics at the regional scale. Apart from the EC-derived LE data, we used the reanalysis data to determine the same on a regional scale. We used surface-level air temperature and relative humidity data to calculate the respective climatology for the study region. Evaporation and transpiration fractions of the moisture fluxes and the soil water content were obtained from satellite-data-driven reanalysis data (GLEAM[25]). We estimated the soil water content at two levels (surface [0–10 cm] level and root zone level; 10–800 cm) using the GLEAM data (Supplementary Fig. 3b).

Meteorological data

The amount of rainfall at Tezpur and Darjeeling sites was obtained from ordinary rain gauges available since 2016. To get the regional scale rainfall information, we have used the TRMM (Tropical Rainfall Measuring Mission) satellite-derived rainfall data[40]. To calculate the rainfall anomaly during the cyclonic events, the rainfall climatology was first prepared from 21-year rainfall data (1998–2018). Then the rainfall climatology was subtracted from the daily rainfall data averaged on a 3-day scale over the study region, including the coastal areas of India and Bangladesh.

To determine the rainfall trend for Assam and Meghalaya of NEI, observed rainfall data for March (1871–2016; available at http://tropmet.res.in) were plotted, and an ordinary regression line was fitted (see Supplementary Note 4). The slope yielded the rate of change of March rainfall for this region.

OLR analysis

NOAA interpolated OLR data were used to characterise the convective activities. First, 10-year OLR climatology (2009–2018) was prepared over the NEI region. Then OLR anomaly was calculated for each year by subtracting the climatology from the respective year which enabled us to compare the extent of convective activities for a different year. We plotted a time-latitude Hovmoller diagram for daily OLR anomaly. Afterwards, the isotopic time profiles were superposed on the Hovmoller diagram to illustrate the synchronisation between the low OLR (i.e., high convection) and the isotopic depletions.

To study the regional-scale moisture transport characteristics, the vertically integrated moisture transport (VIMT) fluxes[41] were calculated for the study region (5°lat × 6°lon) using the following formula[42].

$$\mathrm{VIMT} = \frac{1}{g}\sum_{j=1}^{J} q_j\left(u_j, v_j\right)\Delta p_j \quad (1)$$

where g is the acceleration due to gravity, q_j is the specific humidity (kg kg^{-1}), u_j is the zonal wind speed, v_j is the meridional wind speed at jth pressure level, and Δp_j is the thickness of the jth pressure level. The total number of pressure levels in the consideration for accumulation is J.

The ratio of recycled to the total rainfall (RR)

A fraction of moisture from local ET contributing to local rainfall is called recycling. The ratio between recycled and total rainfall is called the recycling ratio (i.e., recycled rain/total rain). The recycling ratio is estimated by employing the diagnostic model of Eltahir and Bras[43]. The model relies on the basic atmospheric water vapour budget equation and atmospheric parameters (zonal and meridional winds, specific humidity at surface to 200 hPa levels, and ET) as input from ERA5 reanalysis. The observed rainfall is used to calculate the amount of recycled rainfall based on the estimated recycling ratio. The diagnostic model uses two basic assumptions: (i) the rate of change in the storage term is negligible and (ii) the atmospheric water vapour is well mixed. The recycling ratio is calculated at each land

grid point of a selected domain considering species of water vapour molecules, which evaporate within the region (i.e., local) and outside the region (i.e., advection part). The second assumption (i.e., well-mixed) implies that water vapour molecules from advected and local origins have equal probabilities of falling back as precipitation. In contrast, the first assumption holds reasonably well for long-time average cases (i.e., monthly/seasonal). A detailed description of the methodology and simulations is given in Eltahir and Bras[43] and Sujith et al.[44].

Seasonal mean (December–February, March–May, June–August, and September–November) values were calculated for 2014 through 2018, and their climatological pattern was also estimated. It may be noted that the estimation of recycled rainfall in a short time scale introduces significant error, which arises from the basic assumptions of the Eltahir and Bras[43] model. It was found that over the Indian subcontinent, the uncertainty level is negligible if the calculation is done on a seasonal time scale[19,44].

Canopy–atmosphere decoupling coefficient

The canopy–atmosphere decoupling coefficient (Ω) is defined as follows[15]:

$$\Omega = \frac{\lambda + 1}{\lambda + 1 + \frac{G_a}{G_s}} \quad (2)$$

with $\lambda = \delta/\psi$, where δ is the slope of the saturation vapour pressure–air temperature curve (in Pa K^{-1}), ψ is the Psychrometric constant (in Pa K^{-1}), G_a is the aerodynamic conductance of heat (in m s^{-1}), and G_s is the surface conductance to water vapour transport (in m s^{-1}).

There are several methods of calculating G_a and G_s. We have, however, computed them from friction velocity (u^* in m s^{-1}), canopy roughness parameter, displacement height, and Businger stability function. Computations of these parameters are quite involved and require various other parameters. These steps are listed in Deb Burman et al.[26], and we do not repeat those explicitly here as that remains well out of the scope of the present study. Ω is usually considered as a relative measure of environmental control to canopy control on the biosphere–atmosphere water vapour exchange in any ecosystem. Its value ranges within [0,1], with larger values signifying the environmental control dominating the canopy control and vice versa.

DATA AVAILABILITY

The authors declare that all data supporting the findings of this study are available in the Supplementary Information (SI) section. The reanalysis data used are available at https://www.ecmwf.int/en/forecasts/datasets/reanalysis-datasets/era5. The GLEAM data are available at https://www.gleam.eu/. Precipitation isotopic data generated in this study are provided in the SI section: Precipitation Isotope Data File 1–4. Precipitation isotope data source for other sites are mentioned in the SI section. Eddy-covariance-based latent heat flux data are provided in the SI section: Latent heat flux data 5.

Received: 23 January 2021; Accepted: 18 January 2022;
Published online: 09 February 2022

REFERENCES

1. Vuille, M. et al. Stable isotopes in precipitation in the Asian monsoon region. *J. Geophys. Res.* **110**, D23108 (2005).
2. Stewart, M. K. Stable isotope fractionation due to evaporation and isotopic exchange of falling waterdrops: applications to atmospheric processes and evaporation of lakes. *J. Geophys. Res.* **80**, 1133–1146 (1975).
3. Webster, R. C. & Heymsfield, A. J. Water isotope ratios D/H, $^{18}O/^{16}O$, $^{17}O/^{16}O$ in and out of clouds map dehydration pathways. *Science* **302**, 1742–1745 (2003).
4. Deshpande, R. D. et al. Rain-vapour interaction and vapour source identification using stable isotopes from semiarid western India. *J. Geophys. Res. Atmos.* **115**, D23311 (2010).
5. Sinha, N. & Chakraborty, S. Isotopic interaction and source moisture control on the isotopic composition of rainfall over the Bay of Bengal. *Atmos. Res.* **235**, 104760 (2020).
6. Konecky, B. L., Noone, D. C. & Cobb, K. M. The influence of competing hydroclimate processes on stable isotope ratios in tropical rainfall. *Geophys. Res. Lett.* **46**, 1622–1633 (2019).
7. Risi, C., Bony, S. & Vimeux, F. Influence of convective processes on the isotopic composition (δ ^{18}O and δ D) of precipitation and water vapor in the tropics: 2. Physical interpretation of the amount effect. *J. Geophys. Res.* **113**, D19306 (2008).
8. Bhattacharya, S. K. et al. Isotopic variation in Indian Monsoon precipitation: records from Bombay and New Delhi. *Geophys. Res. Lett.* **30**, 2285 (2003).
9. Chakraborty, S. et al. Atmospheric controls on the precipitation isotopes over the Andaman Islands, Bay of Bengal. *Sci. Rep.* **6**, 19555 (2016).
10. Breitenbach, J. F. et al. Strong influence of water vapour source dynamics on stable isotopes in precipitation observed in Southern Meghalaya, NE India. *Earth Planet. Sci. Lett.* **292**, 212–220 (2010).
11. Sinha, N. et al. Isotopic investigation of the moisture transport processes over the Bay of Bengal. *J. Hydrol. X* **2**, 100021 (2019).
12. Jeelani, G. et al. Isotopic composition of daily precipitation along the southern foothills of the Himalayas: impact of marine and continental sources of atmospheric moisture. *Atmos. Chem. Phys.* **18**, 8789–8805 (2018).
13. Cai, Z. & Tian, L. What causes the postmonsoon ^{18}O depletion over Bay of Bengal head and beyond? *Geophys. Res. Lett.* **47**, e2020GL086985 (2020).
14. Gat, J. R., Bowser, C. J. & Kendall, C. The contribution of evaporation from the Great Lakes to the continental atmosphere: estimate based on stable isotope data. *Geophys. Res. Lett.* **21**, 557–560 (1994).
15. Jarvis, P. G. & McNaughton, K. J. Stomatal control of transpiration: scaling up from leaf to region. *Adv. Ecol. Res.* **15**, 1–49 (1986).
16. Sarma, D. et al. Carbon dioxide, water vapour and energy fluxes over a semi-evergreen forest in Assam, Northeast India. *J. Earth Syst. Sci.* **127**, 94 (2018).
17. Deb Burman, P. K. et al. The effect of Indian summer monsoon on the seasonal variation of carbon sequestration by a forest ecosystem over North-East India. *SN Appl. Sci.* **2**, 154 (2020).
18. Sarma, D. et al. Quantifying the net ecosystem exchange at a semi-deciduous forest in northeast India from intra-seasonal to seasonal time scale. *Agric. For. Meteorol.* **314**, 108786 (2022).
19. Choudhury, B. et al. Rapid drying of Northeast India in the last three decades: climate change or natural variability? *J. Geophys. Res. Atmos.* **124**, 227–237 (2019).
20. Gonfiantini, R. et al. The altitude effect on the isotopic composition of tropical rains. *Chem. Geol.* **181**, 147–167 (2001).
21. Mahanta, R., Sarma, R. & Choudhury, A. Heavy rainfall occurrences in northeast India. *Int. J. Climatol.* **33**, 1456–1469 (2013).
22. Tang, K. & Feng, X. The effect of soil hydrology on the oxygen and hydrogen isotopic compositions of plants' source water. *Earth Planet. Sci. Lett.* **185**, 355–367 (2001).
23. Chakraborty, S. et al. Isotopic study of intraseasonal variations of plant transpiration: an alternative means to characterise the dry phases of monsoon. *Sci. Rep.* **8**, 8647 (2018).
24. Pradhan, R., Singh, N. & Singh, R. P. Onset of summer monsoon in Northeast India is preceded by enhanced transpiration. *Sci. Rep.* **9**, 18646 (2019).
25. Miralles, D. G. et al. An application of GLEAM to estimating global evaporation. *Hydrol. Earth Syst. Sci. Dis.* **8**, 1–27 (2011).
26. Deb Burman, P. K. et al. Ecosystem-atmosphere carbon and water exchanges of subtropical evergreen and deciduous forests in India. *For. Ecol. Manage.* **495**, 119371 (2021).
27. Moerman, J. W. et al. Diurnal to interannual rainfall $\delta^{18}O$ variations in northern Borneo driven by regional hydrology. *Earth Planet. Sci. Lett.* **369–370**, 108–119 (2013).
28. Lekshmy, P. et al. ^{18}O depletion in monsoon rain relates to large scale organized convection rather than the amount of rainfall. *Sci. Rep.* **4**, 5661 (2014).
29. Bengtsson, L. The global atmospheric water cycle. *Environ. Res. Lett.* **5**, 5025202 (2010).
30. Webster, P. J. In *The Asian Monsoon* (ed. Wang, B.) Ch. 1 (Springer, 2006).
31. Xi, J. et al. Impacts of intraseasonal SST anomalies on precipitation during Indian Summer Monsoon. *J. Clim.* **28**, 4561–4575 (2015).
32. Derbyshire, S. H. et al. Sensitivity of moist convection to environmental humidity. *Q. J. R. Meteorol. Soc.* **130**, 3055–3079 (2004).
33. Sherwood, S. C. et al. Tropospheric water vapor, convection, and climate. *Rev. Geophys.* **48**, RG2001 (2010).
34. Linné, H. et al. Water vapour flux profiles in the convective boundary layer. *Theor. Appl. Climatol.* **87**, 201–211 (2007).
35. Ranalkar, M. R., Pawar, S. D. & Pradeep Kumar, P. Characteristics of lightning activity in tropical cyclones developed over North Indian Ocean basin during 2010–2015. *Atmos. Res.* **187**, 16–22 (2017).
36. Bajaj, K. et al. Hydrological linkages between different water resources from two contrasting ecosystems of western peninsular India: a stable isotope perspective. *Isot. Environ. Health Stud.* **55**, 532–549 (2019).
37. Reddy, C. S. et al. Nationwide classification of forest types of India using remote sensing and GIS. *Environ. Monit. Assess.* **187**, 777 (2015).
38. Chakraborty, S. et al. In *Assessment of Climate Change over the Indian Region: A Report of the Ministry of Earth Sciences (MoES), Government of India* (eds Krishnan, R. et al.) 73–92 (Springer, 2020).
39. Hersbach, H. et al. The ERA5 global reanalysis. *Q. J. R. Meteorol. Soc.* **146**, 1999–2049 (2020).

40. Huffman, G. J. et al. The TRMM Multisatellite Precipitation Analysis (TMPA): quasi-global, multiyear, combined-sensor precipitation estimates at fine scales. *J. Hydrometeorol.* **8**, 38–55 (2007).
41. Trenberth, K. E., Fasullo, J. T. & Mackaro, J. Atmospheric moisture transports from the ocean to land and global energy flows in reanalyses. *J. Clim.* **24**, 4907–4924 (2011).
42. Godfred-Spenning, C. R. & Reason, C. J. Interannual variability of lower-tropospheric moisture transport during the Australian monsoon. *Int. J. Climatol.* **22**, 509–532 (2002).
43. Eltahir, E. A. B. & Bras, R. L. Precipitation recycling in the Amazon basin. *Q. J. R. Meteorol. Soc.* **120**, 861–880 (1994).
44. Sujith, K. et al. The dominant modes of recycled monsoon rainfall over India. *J. Hydrometeorol.* **18**, 2647–2657 (2017).

ACKNOWLEDGEMENTS

The work is supported by the Earth System Science Organization of the Ministry of Earth Sciences, Govt. of India. We thank the Director, IITM, and R. Krishnan, Executive Director, Center for Climate Change Research, IITM, for their encouragement and support. We thank Masahiro Tanoue for providing the isotopic data of a few sites in Bangladesh. The Department of Forest, Assam, and the security personnel of the Burapahar Range, Assam are acknowledged for their support in running the eddy-covariance facility at Kaziranga National Park. This work is part of a project work of the International Atomic Energy Agency, CRP F31006.

AUTHOR CONTRIBUTIONS

S.C. conceptualised the problem, with input from S.K.S. and P.K.D.B. drafted the manuscript. P.K.D.B., N.S., and A.D. further improved the presentation. S.K.S. and K.S. calculated the recycled ratio. P.K.D.B., N.S., C.M., and A.M. performed the statistical analysis. A.M. and C.M. made reanalysis data interpretation and preparation of graphics. D.S., N.G., and A.B. made the eddy-covariance-based measurements, data curation, processing, and interpretation. A.D. carried out isotopic ratio measurements. D.S., S.M., D.K.P., and S.B. collected rainwater samples at Tezpur, Darjeeling, Kakdweep, and Kolkata, respectively. All the authors read the manuscript.

COMPETING INTERESTS

The authors declare no competing interests.

ADDITIONAL INFORMATION

Supplementary information The online version contains supplementary material available at https://doi.org/10.1038/s41612-022-00231-z.

Correspondence and requests for materials should be addressed to Supriyo Chakraborty.

Reprints and permission information is available at http://www.nature.com/reprints

Publisher's note Springer Nature remains neutral with regard to jurisdictional claims in published maps and institutional affiliations.